

Active and inactive groundwater flow systems: Evidence from a stratified, mountainous terrain

Alan L. Mayo*

Thomas H. Morris

Brigham Young University, Department of Geology, Provo, Utah 84602, USA

Steven Peltier

ExxonMobil, 795 International Boulevard, Houston, Texas 77024, USA

Erik C. Petersen

Petersen Hydrologic, 2695 North 600 East, Lehi, Utah 84043, USA

Kelly Payne

Norwest Corporation, 12th Floor, 136 East South Temple, Salt Lake City, Utah 84111, USA

Laura S. Holman

ExxonMobil, 233 Benmar, Houston, Texas 77060, USA

David Tingey

Brigham Young University, Department of Geology, Provo, Utah 84602, USA

Tamara Fogel

586 Bradford Lane, Evans, Georgia 30809, USA

Brian J. Black

Landmark Graphic Corporation, 15150 Memorial Drive, Houston, Texas 77079, USA

Todd D. Gibbs

Anadarko Petroleum Corporation, 1201 Lake Robbins Drive, The Woodlands, Texas 77380, USA

ABSTRACT

We present a new conceptual model of groundwater flow that describes active and inactive groundwater flow regimes. The model is based on an analysis of interactions between surface water and shallow and deep groundwater in the 240-km-long Wasatch Range and Book Cliffs, Utah, USA. Active zone groundwater flow paths are continuous, responsive to annual recharge and climatic variability, and have groundwater resident times "ages" that become progressively older from recharge to discharge area. Active zone groundwater systems discharge at thousands of springs that issue from the 700+-m-thick, gently dipping, clastic bedrock formations. Springs waters contain appreciable ^3H and anthropogenic ^{14}C .

In contrast, inactive zone groundwater has extremely limited or no communication

with annual recharge and has groundwater mean residence times that do not progressively lengthen along the flow path. Groundwater in the inactive zone may be partitioned, occur as discrete bodies, and may occur in hydraulically isolated regions that do not have hydraulic communication with each other. Inactive zone groundwater is encountered in mines (coal-mines 300–700 m below ground surface) where groundwater discharge rates decline rapidly and the waters have $\delta^3\text{H}$ and $\delta^{18}\text{O}$ compositions that are distinguishable from near surface groundwater. In general, deep waters have no ^3H and have mean ^{14}C residence times of 500 to 20,000 yr (45.9 to 4.9 pmc). Chemical evolution modeling, porosity-permeability core plug analysis, and in-mine hydrographs also indicate hydraulic partitioning.

isotope chemistry, groundwater age, solute chemistry, sedimentary rocks, mountains.

INTRODUCTION

Patterns and mechanisms of groundwater circulation in stratified mountainous terrain are generally not well understood, either conceptually or at the field scale. This occurs because access to deep groundwater is generally limited, the details of subsurface stratigraphic and structural complexities are often poorly defined, and groundwater flow is often fracture-controlled (Committee on Fracture Characterizations of Fluid Flow, 1996).

Hubbert (1940) and Toth (1962, 1963) provided insight into the potential effects of topography and basin geometry on groundwater flow and described the useful concept of local, intermediate, and regional systems. Freeze and Witherspoon (1966, 1967) demonstrated theoretical effects of permeability contrast in adjacent layered strata. Jamieson and Freeze

Keywords: groundwater, conceptual model,

*E-mail: alan_mayo@byu.edu.

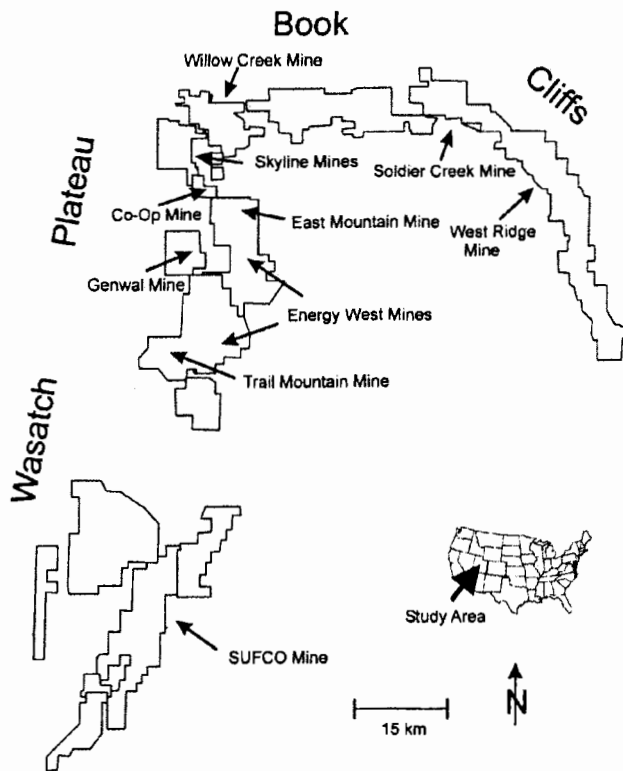


Figure 1. Location of coal mines and coal mine lease areas in Wasatch Plateau and Book Cliffs, Utah. Named mines provided data and underground access for this investigation. SUFCO—Southern Utah Fuel Company.

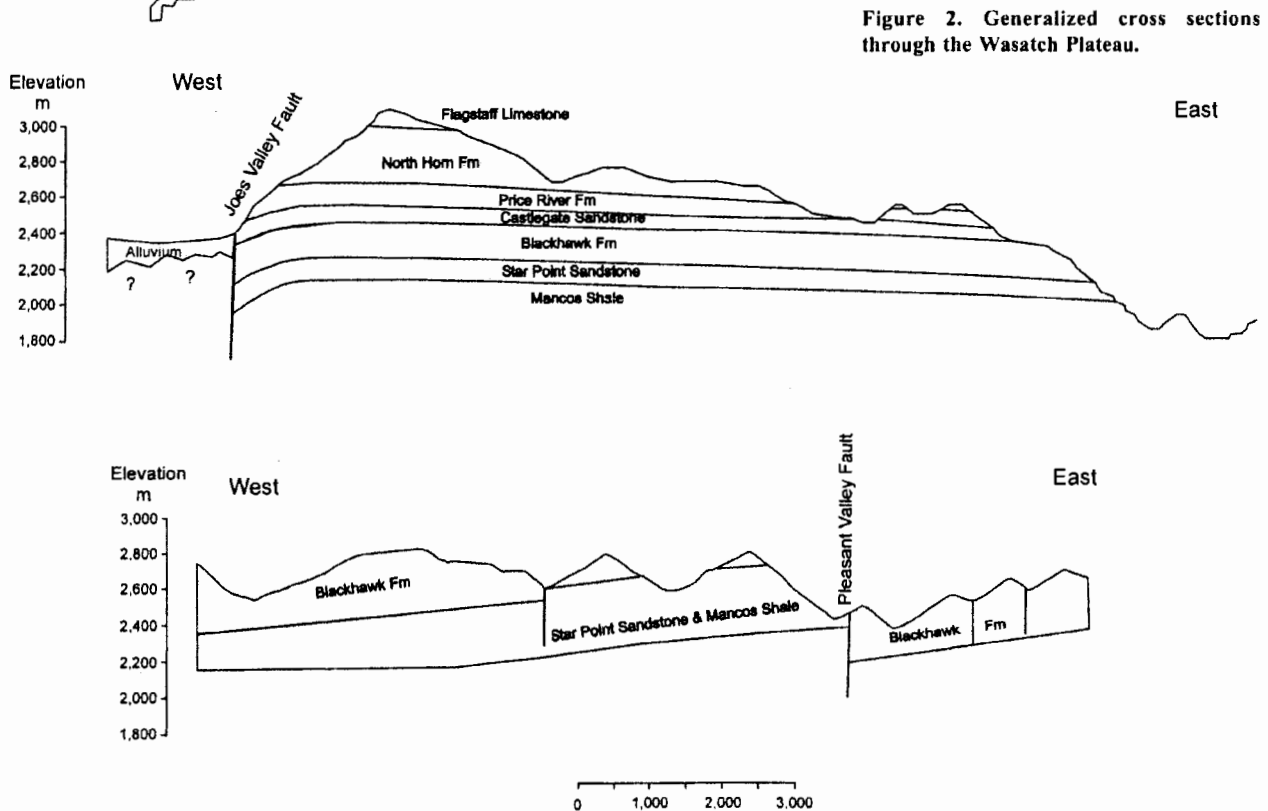


Figure 2. Generalized cross sections through the Wasatch Plateau.

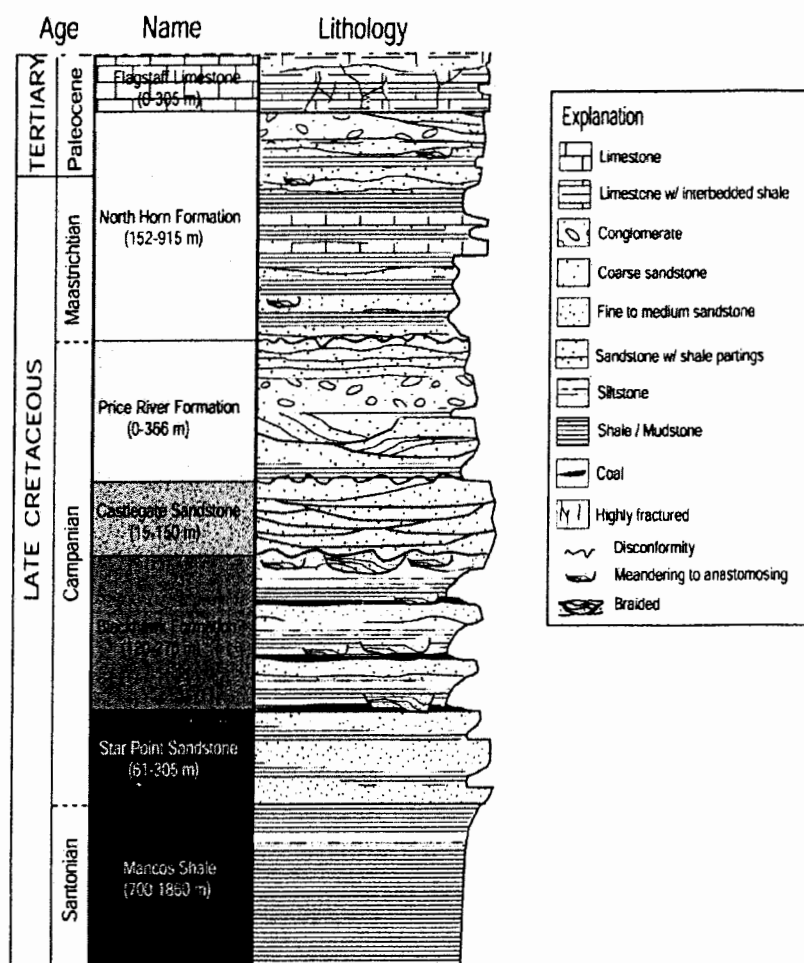


Figure 3. Stratigraphic column of bedrock formations in Wasatch Plateau and Book Cliffs.

TABLE 1. SUMMARY OF AVERAGE DISCHARGE RATES AND SOLUTE COMPOSITIONS OF SPRING AND IN-MINE GROUNDWATERS IN THE WASATCH PLATEAU AND BOOK CLIFFS, UTAH

Formation	Q n	Q (l s ⁻¹)	Solute n	Temp (°C)	Cond us/cm	pH	mg l ⁻¹ TDS	meq l ⁻¹						
								Ca ²⁺	Mg ²⁺	Na ⁺	K ⁺	HCO ₃ ⁻	SO ₄ ⁻	Cl ⁻
Flagstaff	7	0.30	8	6.8	426	7.6	265.4	4.30	1.05	0.24	0.05	4.79	0.63	0.16
std.		0.28		2.1	59	0.4	41.2	1.15	0.36	0.27	0.09	0.59	1.08	0.17
North Horn	60	0.90	78	7.2	593	7.7	343.5	3.27	2.47	1.21	0.04	5.64	0.83	0.44
std.		3.69		3.6	186	0.5	114.9	1.18	0.93	1.46	0.05	1.08	1.13	0.59
Price River	14	0.62	22	6.6	700	7.6	399.5	4.32	2.78	1.03	0.05	6.60	1.25	0.26
std.		0.89		4.7	151	0.4	87.4	1.41	0.85	0.52	0.07	1.02	1.23	0.13
Castlegate	7	5.14	16	11.0	460	7.6	240.4	2.42	1.62	0.36	0.04	3.55	0.57	0.26
std.		11.35		10.3	462	0.6	72.6	0.97	1.02	0.22	0.02	1.63	0.36	0.19
Blackhawk	31	1.20	35	6.7	450	7.3	254.8	3.13	1.45	0.31	0.03	4.06	0.60	0.22
std.		2.84		3.2	238	0.8	99.6	1.02	1.22	0.44	0.04	1.44	0.61	0.30
In-mine			50	11.5	796	7.7	454.4	3.20	2.90	2.80	0.17	7.01	1.47	0.37
std.				2.9	333	0.5	193.8	1.78	1.41	3.50	0.15	2.58	1.61	0.34
Star Point	4	3.42	5	17.0	933	7.4	546.3	5.02	3.75	1.07	0.06	6.45	2.46	0.86
std.		2.63		8.4	188	0.6	150.4	1.39	1.27	0.67	0.04	0.56	1.24	0.68

Note: std—standard deviation.

(1983) and Forster and Smith (1988) evaluated theoretical relationships in well-defined mountainous aquifers that are not constrained by stratigraphic and structural barriers. Although instructive, these studies have limited applicability to groundwater flow in stratified mountainous terrain, because many are based on the limitations of computer simulations, on data collected only at or near the land surface, and on patterns of deep phreatic flow that are largely inferred.

Most stratified mountainous systems consist of numerous stratigraphic and structural features that locally and regionally affect groundwater flow patterns (Allen and Michel, 1998; Janes, 1998; Huntoon, 1981; Mayo et al., 1985; Mayer and Sharp, 1998). In this investigation, we have used geological, physical, chemical, and isotopic data to evaluate interactions between near-surface and 300–700-m-deep groundwater systems in gently dipping stratified bedrock that underlies a 6500 km² mountainous region in Utah, USA (Fig. 1). Because economic coal deposits are mined near the base of the 700+-m-thick section of six bedrock formations, the stratigraphy and structure of the subsurface are relatively well defined. Mine operators have identified thousands of springs and systematically collected discharge and solute data from hundreds of springs. Mine operators have also provided underground access to the geology and deep groundwater systems as much as 13 km laterally into the 240-km-long mountain front.

METHODS OF INVESTIGATION

Solute, isotopic, and hydrographic data were obtained for springs and in-mine discharges from the published literature, quarterly hydrologic reports, and permit applications prepared by various coal mines and unpublished sources.

Major ion chemistry (Ca²⁺, Mg²⁺, Na⁺, K⁺, HCO₃⁻, SO₄²⁻, and Cl⁻) for more than 3000 sampling events was checked for cation/anion balances. Approximately 1930 data sets from 164 springs and 50 in-mine sampling locations had acceptable error balances of ≤ 5%. These data were tabulated according to the formations from which they discharge. Differences in solute compositions of groundwater issuing from each formation and in-mine source were evaluated by normalizing the total dissolved solids data, and by discriminate and z-tests analysis. NETPATH (Plummer et al., 1991) was used to model plausible geochemical reaction pathways.

Isotopic data from surface and in-mine locations include carbon-14 (¹⁴C) and tritium

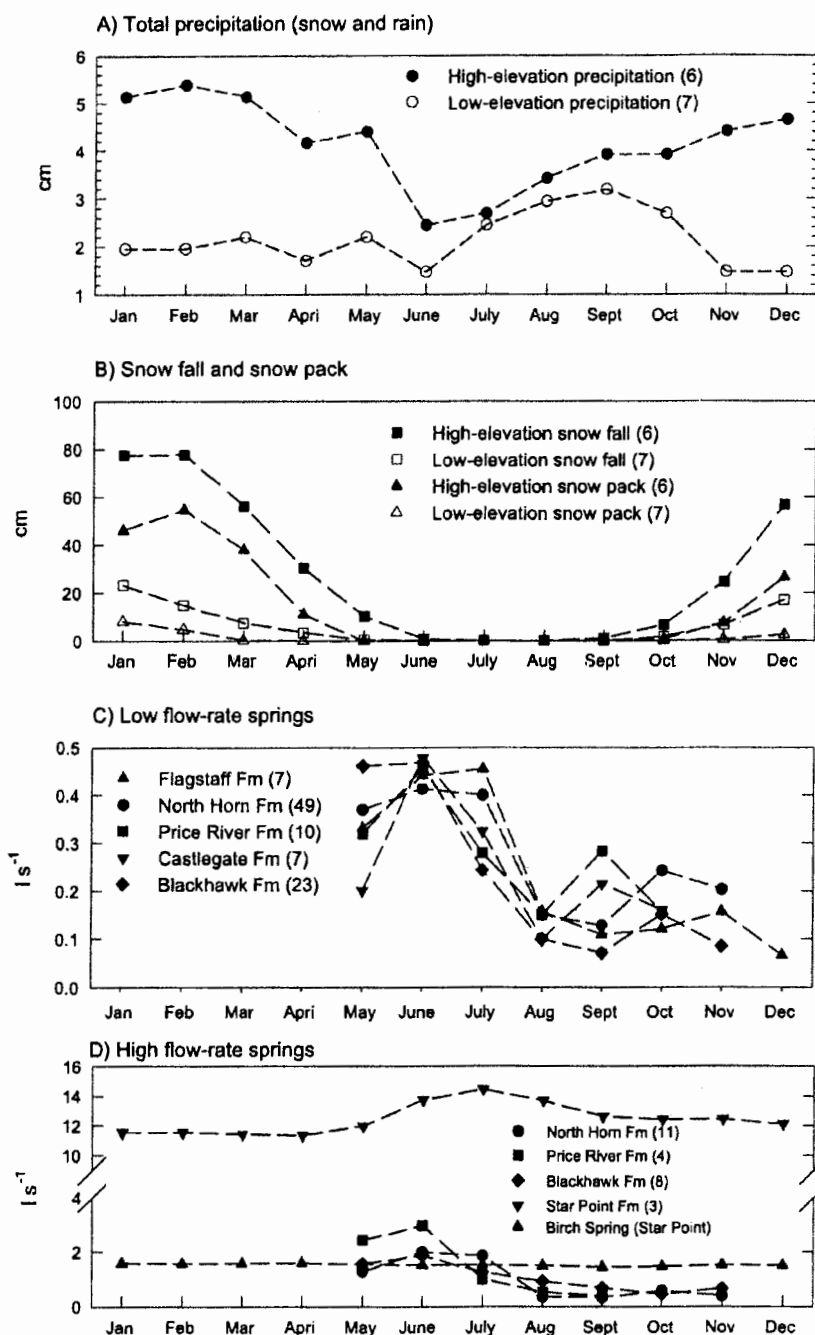


Figure 4. Mean monthly precipitation and spring discharge rates: (A) total precipitation, (B) snowfall and snowpack, (C) discharge rates of low-flow springs, and (D) discharge rates of high-flow springs. Numbers in parentheses are number of precipitation stations (A and B) or number of springs (C and D).

(3H) analyses obtained from 132 sampling locations and 392 δ^2H and $\delta^{18}O$ analyses from 329 sampling locations. Mean ^{14}C residence times were calculated by isotopic mixing (Pearson et al., 1972) and isotopic mixing-exchange (Fontes and Garnier, 1979) models. These models were selected because collectively they accommodate both open and closed systems conditions with abundant carbonate mineral. Calcium carbonate is the prevailing cement in clastic rocks of the Wasatch Plateau and Book Cliffs. Only samples with HCO_3^- $\delta^{13}C > -7\text{‰}$ were modeled. Some samples had $\delta^{13}C$ values as great as $+5\text{‰}$ due to the influence of methane gas. In addition to the measured ^{14}C and $\delta^{13}C$ of the samples, other input parameters were assigned the following values: $\delta^{13}C$ soil gas -18 to -22‰ , $\delta^{13}C$ mineral carbonate 0‰ , ^{14}C soil gas 100 percent modern carbon (pmc), and ^{14}C mineral carbonate 0 pmc. Results of the two methods, including the range of assigned $\delta^{13}C$ soil gas values, were generally within 10% or less of each other for each sample.

Precipitation data were obtained from seven low-elevation (1800–2100 m) and six high-elevation (2100–2500 m) weather stations (Western Region Climate Center, 2001). Low-elevation stations are located near the base of the Wasatch Plateau and Book Cliffs and high-elevation stations are located at elevations between one-half and two-thirds the maximum elevation of the mountains.

Stratigraphic sections were measured in the Castle Gate and Star Point Sandstones to identify sedimentary facies and bounding surfaces between facies. More than 130 core plugs were collected, including multiple cores from bounding surfaces. Porosity and permeability of the cores were analyzed using a TerraTek 8400 dual porosimeter and permeameter. Photomosaics of key outcrops were compiled using Adobe Photoshop 6.0 and Adobe Illustrator 9.0. Bounding surfaces were annotated on the photomosaics in an effort to evaluate the lateral extent and number of bounding surfaces.

SETTING

Geologic Setting

The 2400–2700-m-high Wasatch Plateau and Book Cliffs form a 240-km-long, 16–40-km-wide, arc-shaped upland that rises along imposing erosional escarpments in the northern Colorado Plateau, Utah. The Wasatch Plateau is a northeast-trending mountain range that is stratigraphically and structurally contiguous with the east-west-trending Book

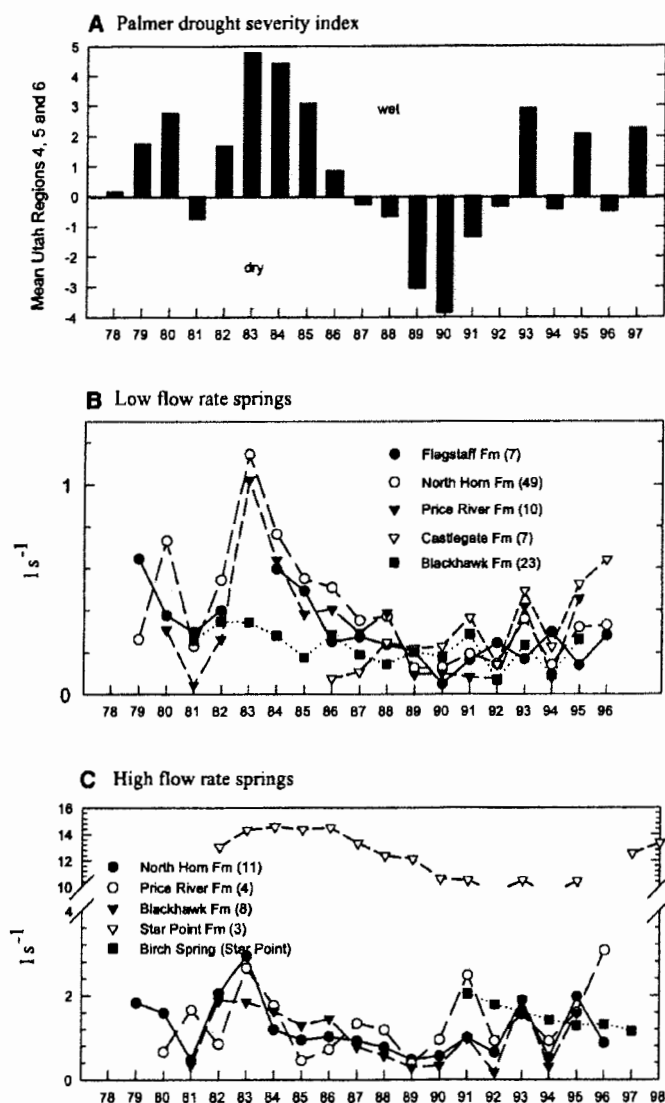


Figure 5. Climate and spring discharge rates for 1978–1987: (A) mean Palmer Hydrologic Drought Index (PHDI) for Utah Regions 4, 5, and 6; (B) low flow-rate springs; and (C) high flow-rate springs. Springs are organized by bedrock formation. Numbers in parentheses are number of springs averaged.

Cliffs. The prominent features of the eastern and southern fronts of the Wasatch Plateau and Book Cliffs, respectively, are 460–915-m-high, stair-stepped cliff faces. Ancillary canyons and reentrants, through which streams drain the interior uplands, cut the cliff faces.

The bedrock, which dips 2–5° east, is broken by high-angle normal faults that parallel the length of the plateau (Fig. 2). Some of the faulting has resulted in narrow elongate grabens internal to the plateau (Witkind and

Weiss, 1991); elsewhere, normal faulting does not have a pronounced topographic expression. A large fault-block basin bounds the Wasatch Plateau to the west. The Book Cliffs mark the southern edge of the uplifted Uinta Basin. Bedrock that crops out in the cliff faces dip beneath younger Uinta Basin sediments to the north.

Six Upper Cretaceous through Lower Tertiary water-bearing formations, with an aggregate thickness as much as 2311 m, occur in

the region (Fig. 3). The formations include the Flagstaff Limestone, North Horn Formation, and four formations (Price River Formation, Castlegate Sandstone, Blackhawk Formation, and Star Point Sandstone) of the Mesa Verde Group. The rocks were deposited along the edges of the western shoreline of the Cretaceous Interior Seaway on top of marine mud of the Mancos Shale (Johnson, 1978; Stanley and Colinson, 1979; Knowles, 1983; Hintze, 1988; Chan and Phaff, 1991; Franczk and Pittman, 1991; Van Wagoner et al., 1990). The highlands were the result of the Sevier Orogeny foreland thrust belt. Sediment from the highlands was shed eastward through a variety of depositional systems, including alluvial plains containing a variety of fluvial types, coastal to delta plains, and deltaic to marine shoreface deposits. Through time, the depositional systems prograded eastward, creating an overall upward-coarsening succession of Upper Cretaceous rocks.

In the latest Cretaceous (Upper Maastrichtian) and Paleocene, an intermountain basin developed in the region (Franczk and Pittman, 1991). The basin filled with low-gradient, meandering stream and over-bank flood-plain deposits of the North Horn Formation. These deposits give way upward to lacustrine carbonates of the Flagstaff Limestone (Fig. 3; Garner and Morris, 1996). Because of the stair-step erosional surface of the Wasatch Plateau and Book Cliffs, the cap rock ranges from the highly fractured Flagstaff Limestone to the Blackhawk Formation.

Economic coal seams occur in the lower portion of the Blackhawk Formation. As much as 1860 m of nonwater-bearing marine Mancos Shale interfingers with and underlies the Star Point Sandstone and Blackhawk Formation in the study area.

Climate

Mean annual precipitation varies between 25 and 90 cm, depending on elevation (Western Region Climate Center, 2001; Utah State University Climate Center, 2001). Most low-elevation precipitation falls as rain during the summer, whereas ~50% of the high-elevation precipitation falls as snow during the winter (Fig. 4, A and B). In January and February, the mean snowpack depth at high-elevation weather stations is ~0.75 m and depths as great as 1.5 m are common in the higher upland areas of the Wasatch Plateau (>2500 m) where weather stations do not exist.

The mean air temperature is below freezing between November and March. Mean nighttime minimum temperatures are below freezing



Figure 6. Bedding discharge in North Horn Formation. Discharge is fracture-controlled and occurs in discrete locations along bedding surfaces.

GROUNDWATER DISCHARGE

Spring Discharges

Based on a field examination of the geology of more than 50 springs, we found five instances of shallow groundwater discharge: along bedding surfaces, along fracture and bedding surfaces, regolith-soil underflow, slump-block flow, and fault-zone discharge. Most perennial springs discharge along bedding surfaces (Fig. 6); however, the regolith-soil underflow type is the dominant ephemeral spring. Although fault-related springs are uncommon, damage zone discharge is responsible for some notable springs in the Star Point Sandstone. Fault-related springs often have a muted response to seasonal recharge.

Discharge rate data for 123 springs for which long-term records are available have been analyzed for seasonal and climatic recharge effects. These springs have been organized according to bedrock lithology (Table 1). About 80% of the springs are classified as low-

ing between October and May. The snowpack begins melting at the lower elevations in March, and melting is usually complete by the end of May.

Mean Palmer Hydrologic Drought Index for Utah regions 4, 5, and 6 (National Climatic Data Center, 2001a, b) and precipitation data

from nearby weather stations for the years 1978–1997 indicate that the amount of moisture available for potential groundwater recharge is cyclical (Fig. 5, A and B). The years 1979–1986 were relatively wet, 1987–1992 were relatively dry, and both wet and dry years have occurred since then.

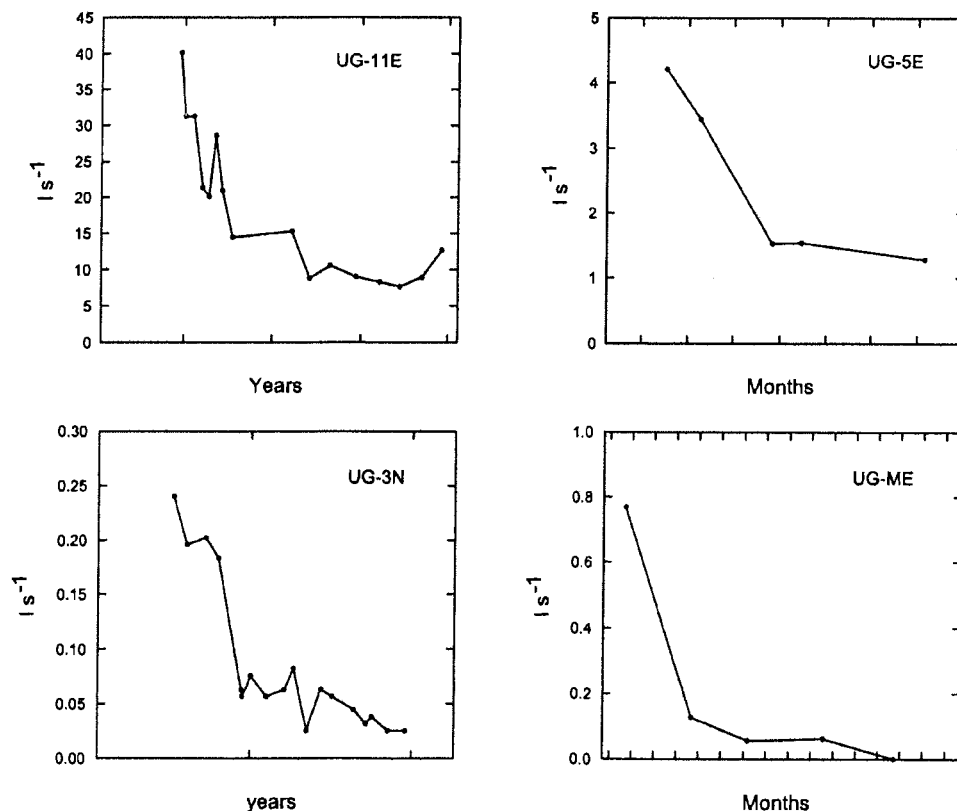


Figure 7. Typical hydrographs of in-mine roof drips.

discharge rate (mean discharge $< 0.65 \text{ l s}^{-1}$), and $\sim 20\%$ are classified as high-discharge rate (Fig. 4, C and D; and Fig. 5, B and C). In Table 1, the large standard deviations in discharge rate result from seasonal and climatic variability.

All spring types except for high-discharge springs in the Star Point Sandstone have similar bimodal discharge characteristics and are influenced by seasonal recharge (Fig. 4, C and 4D). Mean discharge rates in the spring and early summer are generally two to four times as great as are discharge rates in the late summer and fall (Fig. 4D). The elevated discharge rates reflect snowmelt-induced recharge and late spring and early summer rain. There is a one- to two-month lag between the end of snowmelt and the peak of spring discharge rates (Fig. 4, B and C). We interpret this lag to travel times between recharge and discharge areas (i.e., delayed drainage). There is also a lag between the beginning of increased summer precipitation and summer discharge rates. Springs generally exhibit a decrease in discharge in the late fall and early winter as the precipitation turns to snow. Birch Spring in the Star Point Sandstone is the only spring not affected by seasonal precipitation (Fig. 4D).

Discharge rates of both low- and high-discharge springs are also affected by multi-year climate variations. Flagstaff, Northhorn, Price River, and Castlegate Formation springs generally exhibit rapid response to wet and dry periods, whereas Blackhawk and Star Point Formation springs have a more muted response.

In-Mine Groundwater Discharges

The network of nearly horizontal underground mine openings provides an opportunity to examine and monitor groundwater responses in deep groundwater systems. These interconnected tunnels and longwall-mined areas may be thought of as large-diameter horizontal wells. Although openings are as much as 700 m below ground surface, most openings encounter little water and dry regions commonly occur. Dust suppression is required in many mine openings. Most groundwater inflows are from the mine roof, emanating from roof-bolt holes and small fractures. In some mines, water may locally discharge from the mine floor. Occasionally, substantial inflows issue from fault-related damage zone fractures (Mayo and Kuntz, 2000). Roof inflows are usually from sandstone channels in the Blackhawk Formation and floor inflows are usually from the Star Point Sandstone.

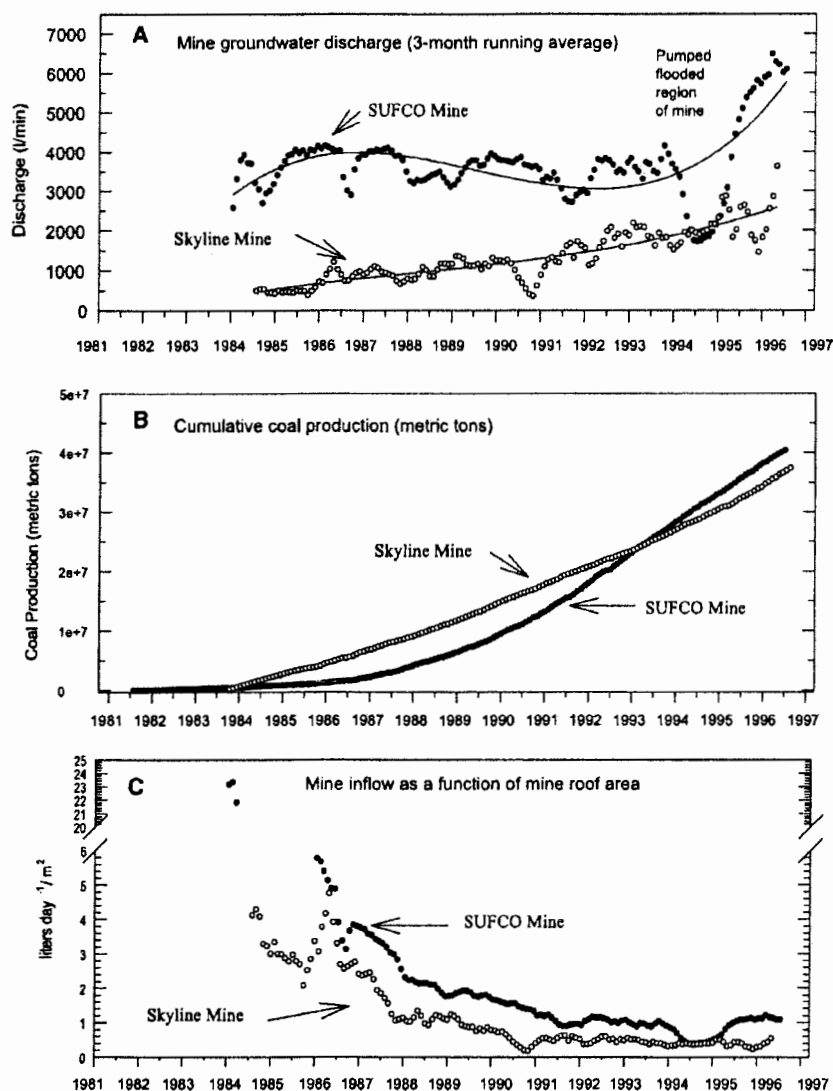


Figure 8. Relationships between (A) in-mine groundwater discharge rate, (B) coal production, and (C) area of exposed mine roof.

Mine inflows do not exhibit seasonal or climatic responses. Most roof drips are only reported anecdotally, as they dry up within a few days to a few weeks. The typical response of longer-term mine inflows is an initial rapid decline followed by a slower decline and ultimate extinction (Fig. 7).

The overall responses of in-mine groundwater inflows are consistent with hydrographs of individual roof drips. Groundwater inflows into the Skyline and Southern Utah Fuel Company (SUFCO) Mines illustrate this relationship (Fig. 8). Discharge into the SUFCO Mine was relatively constant between 1984 and

1997 (Fig. 8A). The major decrease in mid-1994 followed by the increase in 1995 was the result of mine storage of groundwater followed by mine pumping. The discharge rate in the Skyline Mine has been generally less than in the SUFCO mine, but it has gradually increased over time. Average monthly coal production from each mine was $\sim 240,000$ metric tons between 1984 and 1997. Cumulative production is shown in Figure 8B. The steady decline in groundwater inflow rates per unit of mined roof area (Fig. 8C) indicates that groundwater inflow is not steady state. Because mine workings are essentially horizontal

and are parallel to bedding, the decline in inflow is attributed to rapid dewatering of old mine workings.

The similarity of the SUFCO and Skyline Mines dewatering trends (Fig. 8C) indicates that groundwater systems that drain into the mines have similar properties. This is particularly significant in that the mines are located more than 50 km from each other and the surfaces above the mines have different climates. SUFCO and Skyline Mines have mean annual precipitation of 38.1 and 60.7 cm/yr, respectively.

HYDROGEOCHEMISTRY

Solute Compositions

Mean solute compositions of spring and in-mine groundwater are listed in Table 1, and mean total dissolved solid contents are shown in Figure 9. Most groundwaters are of the $\text{Ca}^{2+}\text{-Mg}^{2+}\text{-HCO}_3^-$ type; however, North Horn and in-mine waters have appreciable Na^+ contents due to ion exchange, and Star Point waters have appreciable SO_4^{2-} and Cl^- contents due to contact with primary evaporite minerals in the underlying and interfingering Mancos Shale.

Two statistical procedures, z-test and discriminant analysis (Ostle and Malone, 1988), were used to determine if groundwater chemistries from each stratigraphic unit and in-mine waters are chemically distinguishable from each other. Z-tests were performed on the regional data set to compare the mean total dissolved solids and major ion chemistry of groundwater samples from adjacent formations at the 95% confidence interval (Table 2). A z-score of ± 1.4 , for example, represents only an 8% probability that the means of the two populations are the same and a z-score of ± 6.5 represents only a 4.64e-11% probability that the means of the two populations are the same. The z-test results indicate that the means of all groundwater solute compositions of adjacent formations are statistically different from each other.

Discriminant analyses were performed on the entire regional data set and on data sets from specific mining areas. Using the entire regional data set, Blackhawk Formation groundwater has the lowest probability of being correctly identified as Blackhawk Formation groundwater (31.75%), whereas Flagstaff Limestone groundwater has the highest probability (79.69%) of being correctly identified (Table 3). The low probability of Blackhawk Formation groundwater means that the variability of Blackhawk waters is so great that

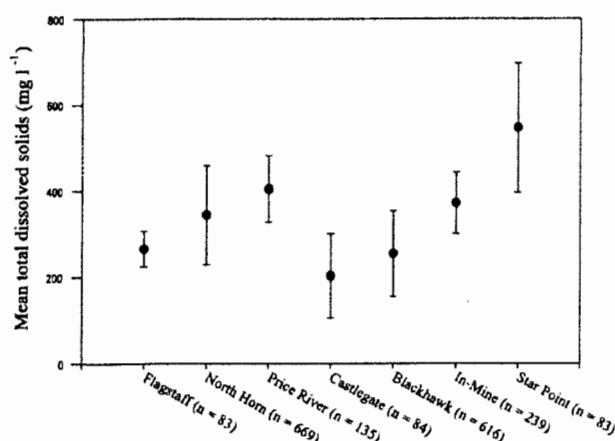


Figure 9. Mean total dissolved solid values of all measurement events for springs from and in-mine sources grouped according to bedrock lithology. Error bars represent 1 standard deviation.

TABLE 2. TWO SAMPLE MEANS Z-TEST STATISTICS FOR COMPOSITIONS OF SPRING AND IN-MINE GROUNDWATERS

Parameter	Flagstaff-North Horn	North Horn-Price River	Price River-Castlegate	Castlegate-Blackhawk	Blackhawk-Star Point	Blackhawk in-mine-Blackhawk spring
TDS	-11.33	-5.60	12.05	-1.31	-16.54	27.06
Ca	6.48	-6.70	9.77	-5.13	-11.47	0.55
Mg	-24.18	-3.38	7.13	1.14	-15.02	15.69
Na	-14.48	2.41	11.13	1.49	-9.66	15.69
HCO ₃ ⁻	-10.00	-8.54	12.48	-2.16	-26.90	27.75
SO ₄ ²⁻	-1.68	-2.92	5.11	-0.44	-12.94	9.97

Note: Conditions of statistical analysis. $H_0: \mu = x$, $H_a: \mu = X$, $\alpha = 0.05$. Z-tests are based on the entire data set and are not location specific.

TABLE 3. SUMMARY OF DISCRIMINANT ANALYSIS, INCLUDING PROBABILITY COEFFICIENTS FOR THE ENTIRE DATA SET, REGARDLESS OF LOCATION

	Flagstaff	North Horn	Price River	Castlegate	Blackhawk	Star Point	In-mine	Total (%)
Flagstaff	51 79.69*	2 3.13	2 3.13	1 1.56	8 12.5	0 0	0 0	64 100
North Horn	61 9.06	341 50.67	67 9.96	45 6.69	61 9.06	59 8.77	39 5.79	673 100
Price River	14 14.29	6 6.12	61 62.24	2 2.04	3 3.06	6 6.12	6 6.12	98 100
Castlegate	1 1.85	14 25.93	4 7.41	32 59.26	3 5.56	0 0	0 0	54 100
Blackhawk	123 20.13	82 13.42	45 7.36	145 23.73†	194 31.75	9 1.47	13 2.13	611 100
Star Point	4 5.13	6 7.69	25 32.05	0 0	0 0	42 53.85	1 1.28	78 100
In-mine	4 1.43	26 9.32	70 25.09	33 11.83	8 2.87	24 8.6	114 40.86	279 100
Total	258	477	274	258	277	140	173	1857
Percent	13.89	25.69	14.75	13.89	14.92	7.54	9.32	100
Error Rate	0.6825	0.4074	0.2031	0.4933	0.3776	0.4615	0.5914	0.4595
Priors	0.1429	0.1429	0.1429	0.1429	0.1429	0.1429	0.1429	

*Table showing the results of regional discriminant analysis. The first set of numbers in each row is the number of sample categories having the chemistry of the formation listed in the column. The second set of numbers is the probability that a sample will be designated as belonging to the formation listed in the column. Groundwaters are initially assumed to be assigned to their correct formation and probability coefficients and are generated under that assumption. An equation is generated describing each formation and each sample's data are evaluated for each equation. The sampling event is then categorized as the equation that yields the highest value. Percentages of sampling events correctly categorized are then tabulated for each formation. Probabilities for correct categorization as well as probabilities for incorrect categorization are displayed for each formation.

†Probability that a water initially designated as Flagstaff will be categorized as Flagstaff.

‡Probability that a water initially designated as Blackhawk will be categorized as Castlegate.

individual spring discharges are often not statistically distinct from those in other formations. The remainder of the formation groundwater has only a 50–60% probability of being correctly categorized, and the overall probability of any sampling event of being correctly categorized is 45.9%. This means that with the exception of the Flagstaff Limestone, groundwaters issuing from these formations are only somewhat chemically distinct when viewed regionally. However, it is significant that in-mine Blackhawk groundwater has only a 2.9 and 8.6% probability of being identified as Blackhawk or Star Point spring water, respectively.

On a mine-by-mine basis, most formation groundwater had a 70–90% probability of being correctly categorized, and many had probabilities of 90–100%. The general low probabilities of the regional analysis and the high probabilities of mine-by-mine analyses are attributed to the spatial variability of the chemistry and mineralogy of the bedrock formations. Groundwater residence times are not considered to be a factor in the spatial variability, because most of the samples are from bedrock sources, many of which were sampled during times of low discharge. Thus, total dissolved solids and chemistry cannot categorize springs on a regional basis. However, solute chemistry is a good indication of bedrock type in each mine area.

To evaluate the potential for vertical groundwater migration between formations, the computer code NETPATH (Plummer et al., 1991) was used to evaluate plausible chemical evolutionary pathways at each mining area. Two chemical evolution scenarios were evaluated for each mining area: recharge to formation and formation to formation. Each model was based on the water chemistry of each mining area. Recharge to formation models assume: (1) groundwater issuing from springs is recharged from precipitation at the outcrop of the formation. Precipitation was assigned the mean composition of Wasatch Range snow (unpublished data), and (2) formation water was assigned the mean composition of spring water issuing from the formation at each mine area. Formation to formation models assume: (1) groundwater in the overlying formation has the mean composition of springs issuing from the formation, (2) the groundwater in the overlying formation is chemically fully evolved, and (3) the groundwater flows through the underlying formation before discharging. Formation to formation models used the mean compositions of specific formation groundwaters in each mine area.

TABLE 4. RESULTS OF NETPATH MODELING OF GEOCHEMICAL EVOLUTION FROM PRECIPITATION TO MEAN COMPOSITION OF GROUNDWATER IN EACH FORMATION AT EACH MINE SITE

Initial water Final water	Precip. Flagstaff	Precip. North Horn	Precip. Price River	Precip. Castlegate	Precip. Blackhawk	Precip. Star Point
Co-Op Mine						
Calcite	0.65					
CO ₂	2.08	2.51			2.02	
Dolomite	0.90	0.97			1.09	
Exchange	-0.35	-0.38			-0.52	
Gypsum	0.03	0.05			0.05	
K-mica	0.02	0.05			0.03	
Plagioclase AN38		0.86			0.14	
East Mountain Mine						
Calcite	1.32				-1.50	
CO ₂	1.75	2.60	3.33		1.94	
Dolomite	0.48	1.11	1.42		1.79	
Exchange		0.02	0.19			
Gypsum	0.30	0.38	0.66		0.78	
K-mica	0.04	0.04	0.05		0.07	
Plagioclase AN38	0.11	0.75	0.74		0.84	
Genwall Mine						
Calcite			-0.86		-0.60	-3.46
CO ₂		1.55	1.18		4.89	2.22
Dolomite		0.54	1.48		1.65	3.73
Exchange		-0.30			-0.02	
Gypsum		0.14	0.26		0.38	0.74
K-mica		0.02	0.11		0.03	0.14
Plagioclase AN38		0.80	0.42			0.46
SUFCO Mine						
Calcite				0.18	0.07	-0.51
CO ₂		4.31	3.70	0.58	1.57	3.09
Dolomite		1.33	1.49	0.44	1.00	1.92
Exchange		1.19	1.26	0.24	0.39	0.14
Gypsum		1.00	1.28	0.22	0.47	1.32
K-mica		0.07	0.08	0.03	0.04	0.07
Plagioclase AN38		1.60	1.08	0.16	0.05	
Trail Mountain Mine						
Calcite		-1.56	1.40	0.74	-0.74	
CO ₂		3.53	1.88	2.51	2.41	
Dolomite		1.60	0.73	1.11	1.69	
Exchange						
Gypsum		0.49	0.04	0.28	0.62	
K-mica		0.04	0.02	0.02	0.03	
Plagioclase AN38		1.03	0.11	0.28	0.41	
US Fuel Mine						
Calcite		0.81		-0.89	-0.46	
CO ₂		1.40		1.76	2.39	
Dolomite		0.75		1.82	1.80	
Exchange		0.02		0.05	0.14	
Gypsum		0.09		1.00	0.56	
K-mica		0.01		0.04	0.03	
Plagioclase AN38					0.29	
Willow Creek Mine						
Calcite		0.91		0.84	0.16	0.79
CO ₂		0.61		1.13	1.27	2.44
Dolomite		0.4		0.43	1.15	0.77
Exchange						
Gypsum		0.26		0.10	0.29	0.33
K-mica		0.01		0.00	0.00	0.02
Plagioclase AN38		0.09		0.11	0.16	0.12

Note: Results in mmol/L. Empty cell = no data from formation water or model result did not include the mineral phase. Positive results indicate mineral dissolution or gas consumption. Negative values indicate mineral precipitation or gas production.

A series of progressively complex model runs was performed. The first models included calcite, dolomite, carbonic acid, gypsum, clay-ion exchange, and zeolite-ion exchange. Plagioclase (AN38) and potassium mica were added to subsequent model runs. All of the mineral phases except zeolite occur in all bedrock formations. Zeolite is restricted to the Blackhawk Formation. Tables 4 and 5 show the NETPATH results for recharge-formation

and formation-formation reactions, respectively. Similar results were obtained for the model runs without silicate mineral phases. In the tables, a positive value indicates dissolution and a negative value indicates precipitation.

In all cases, plausible reactions were modeled for recharge-formation groundwater flow paths for each mine area (Table 4). Attempts to model formation-formation chemical reactions were less successful (Table 5). Assuming

TABLE 5. RESULTS OF NETPATH MODELING OF GEOCHEMICAL EVOLUTION OF MEAN COMPOSITION OF FORMATION GROUNDWATER TO MEAN COMPOSITION OF UNDERLYING FORMATION GROUNDWATER AT EACH MINE SITE

Initial water Final water	Flagstaff North Horn	North Horn Price River	Price River Castlegate	Castlegate Blackhawk	Blackhawk Star Point
Co-Op Mine					
Calcite	nm				
CO ₂	nm				
Dolomite	nm				
Exchange	nm				
Gypsum	nm				
K-mica	nm				
Plagioclase AN38	nm				
East Mountain Mine					
Calcite	-0.88	-0.01			
CO ₂	0.88	0.74			
Dolomite	0.64	0.31			
Exchange	0.22	0.17			
Gypsum	0.08	0.28			
K-mica	ci	0.01			
Plagioclase AN38					
Genwall Mine					
Calcite		nm			nm
CO ₂		nm			nm
Dolomite		nm			nm
Exchange		nm			nm
Gypsum		nm			nm
K-mica		nm			nm
Plagioclase AN38		nm			nm
SUFCO Mine					
Calcite		nm	nm	nm	0.45
CO ₂		nm	nm	nm	1.83
Dolomite		nm	nm	nm	0.91
Exchange		nm	nm	nm	
Gypsum		nm	nm	nm	0.85
K-mica		nm	nm	nm	0.03
Plagioclase AN38		nm	nm	nm	0.39
Trail Mountain Mine					
Calcite		nm	-5.54	nm	
CO ₂		nm	0.53	nm	
Dolomite		nm	0.39	nm	
Exchange		nm	ci	nm	
Gypsum		nm	ci	nm	
K-mica		nm	0.00	nm	
Plagioclase AN38		nm		nm	
US Fuel Mine					
Calcite				nm	
CO ₂				nm	
Dolomite				nm	
Exchange				nm	
Gypsum				nm	
K-mica				nm	
Plagioclase AN38				nm	
Willow Creek Mine					
Calcite				-0.67	nm
CO ₂				0.13	nm
Dolomite				0.72	nm
Exchange					nm
Gypsum				0.19	nm
K-mica					nm
Plagioclase AN38				0.05	nm

Note: Result in mmol/L. ci—models returned only by ignoring one or more constraints—reaction not plausible; nm—no models returned; empty cell—no data or model result did not include mineral phase. Flow paths based on the mean chemical composition of formation groundwater at each mine. Positive results indicate mineral dissolution or gas consumption at each mine. Positive results indicate mineral dissolution or gas consumption. Negative values indicate mineral precipitation.

the overlying formation groundwater is fully evolved, NETPATH results suggest that the vertical movement of groundwater between formations is limited and may not occur at many locations. Of the 15 model runs, 10 were completely unsuccessful and three were successful by ignoring one or more constraints. Blackhawk in-mine models, not

shown, were also unsuccessful. We attribute the failure of these models to the oxidation of pyrite and fugitive longwall-mining machine emulsion fluid that were not included in the models, because necessary $\delta^{13}\text{C}$ and $\delta^{34}\text{S}$ data are not available. Such reactions have been successfully modeled elsewhere in the Wasatch Plateau (Mayo et al., 2000).

Isotopic Compositions

The stable isotopic compositions of $\delta^2\text{H}$ and $\delta^{18}\text{O}$ were analyzed on a regional and mine-by-mine basis (Table 6). Isotopic compositions of waters in the more arid Book Cliffs tend to be heavier than the isotopic compositions of waters in the more humid Wasatch Plateau (Fig. 10). All of the waters plot near the meteoric water line, suggesting a meteoric origin.

At most mine locations, the average isotopic compositions of stream and spring waters are similar, suggesting similar histories (Fig. 11). Except for the Willow Creek and Energy West Mines, the mean compositions of in-mine groundwaters are 0.8–1.2‰ lighter in $\delta^{18}\text{O}$ and 6.0 to 8.9‰ lighter in $\delta^2\text{H}$ than their corresponding surface water counterparts. Willow Creek in-mine waters were collected from roof drips located near the mine entrance. Isotopic differences between spring and in-mine groundwaters indicate that near-surface groundwater does not have rapid hydraulic communication with deep in-mine water. The isotopic depletion of in-mine waters is likely the result of paleo-recharge during cooler climate conditions.

Radiogenic isotopic compositions indicate that spring and in-mine groundwaters have fundamentally different travel times. In-mine groundwater and fault-related springs typically have zero or near zero ^3H contents and mean ^{14}C residence times ("ages") of 500 to 20,000 yr (Fig. 12). Almost all springs contain anthropogenic ^{14}C (i.e., ≥ 50 pmc) and have ^3H contents of 5–30 tritium unit (TU). A few samples contain components of both old groundwater and modern water (i.e., they have ^{14}C and $\delta^{13}\text{C}$ contents that permit the calculation of a ^{14}C -age and contain measurable ^3H). These samples include three Blackhawk Formation springs, most of the wells, and a few in-mine fault and other in-mine samples.

GROUNDWATER FLOW MECHANISMS

Spring and in-mine discharge data, solute and isotopic compositions, and groundwater ages provide evidence that deep groundwater is chemically and isotopically different than near-surface groundwater. These differences suggest restricted hydraulic communication between shallow and deep groundwater systems and beg the question: Why does this restriction occur, and how does deep groundwater move within the interior of the plateau? To address this question, we examined the stratigraphy of the sedimentary succession, studied

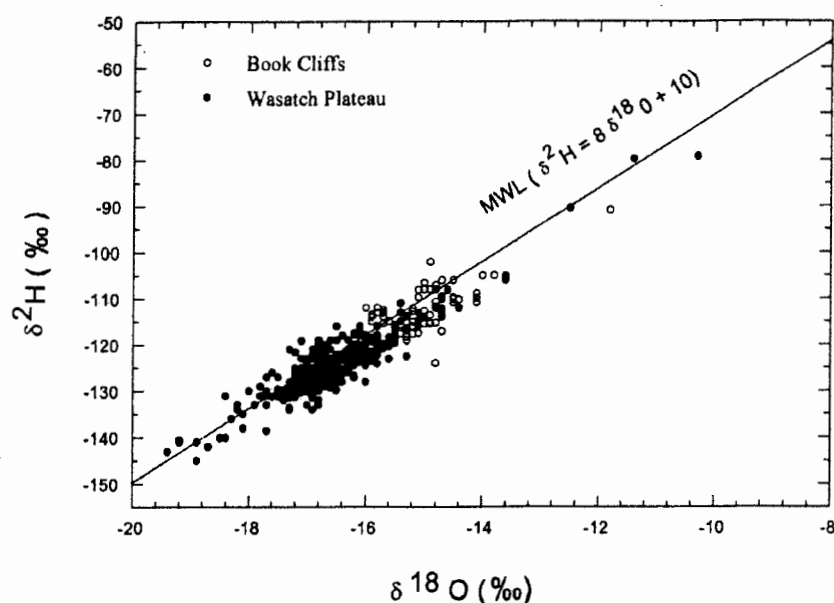


Figure 10. Scatter plot of stable isotopic compositions of all surface water and groundwater in Wasatch Plateau and Book Cliffs, Utah.

the two most laterally extensive reservoir-quality sandstone deposits in the region, and examined in-mine and surface-fault related groundwater inflows.

The sedimentary succession includes a heterogeneous combination aquifer-quality (i.e., water-bearing) sandstone and fractured limestone as well as nonwater-bearing shale, mudstone, siltstone, and nonfractured limestone (Chan and Pfaff, 1991; Kamola and Huntoon, 1995; Miall, 1993; Morris and Mayo, 2000). Above the Star Point Sandstone, most of the water-bearing rocks are channel-fill deposits and marine shoreface sandstone (Fig. 13). Within the aquifer-quality rocks, internal bounding surfaces (e.g., fluvial channel scours and mud drapes of multi-lateral accretion sets) and facies changes create additional horizontal and vertical barriers and baffles to fluid flow. Hence, lithologic heterogeneity at several scales restricts the potential for vertical and horizontal movement of water.

The North Horn Formation illustrates the potential for fine-grained sediments to limit vertical groundwater movement where laterally continuous mudstone beds are abundant. Aquifer-quality fractured limestone of the overlying Flagstaff Limestone and exposed reservoir-quality sandstones within the North

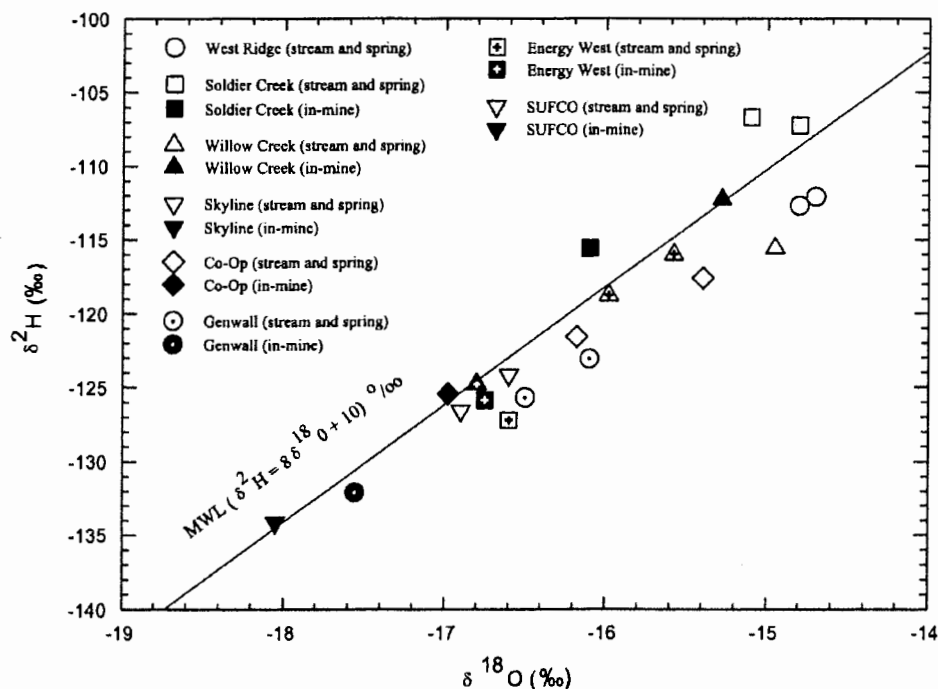


Figure 11. Scatter plot of mean stable isotopic compositions of surface-water, groundwater, and in-mine groundwater samples in Wasatch Plateau and Book Cliffs. Data are sorted according to mine locations, SUFCO—Southern Utah Fuel Company.

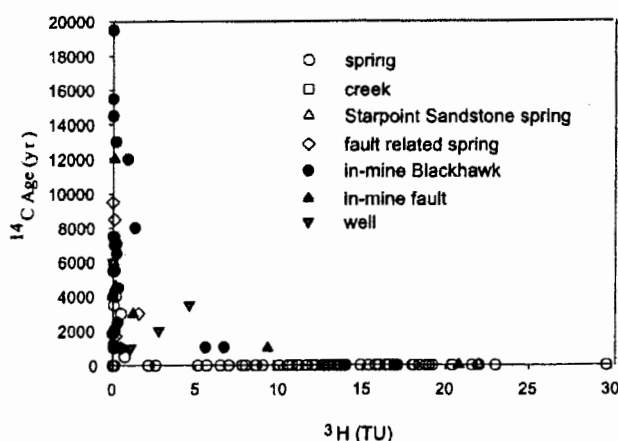


Figure 12. Scatter plot of ^{14}C mean residence times ("age") versus ^3H contents of surface water and groundwater.

Horn Formation provide vertical avenues for water movement. Where vertically flowing water encounters the lower permeability beds, vertical movement is impeded. This water becomes perched and flows laterally to surface outcrops to discharge as seeps or springs (Fig. 6). Such low-permeability horizons act as a "roof" to underlying formations.

Both low-permeability regions and unsaturated aquifer-quality sandstones occur in the coal-bearing Blackhawk Formation. Lines

(1985) found hydraulic conductivities as low as 0.02 to 0.2 millidarcy (md) in cores of shale and siltstone and found one Blackhawk Formation Shale sample to be effectively impermeable under a hydraulic pressure of 5000 psi. Aquifer-quality rocks in the Blackhawk Formation occur in complex anastomosing to braided fluvial sandstone channels that are separated by abundant mudstones (Miall, 1993). Such channels are responsible for most mine inflows. These channel systems have

been well mapped in the Energy West Mine (Fig. 14). In that mine, we installed a series of 4.5- to 7.5-m-long vertical wells into the recently exposed sandstone roof. Maximum water depth in the wells was ~1.5 m, demonstrating that the sandstone channel was not fully saturated and contained a perched, unconfined groundwater system. Extensive exploratory drilling by mining companies indicates that channel complexes are common, both vertically and horizontally, throughout the Blackhawk Formation.

Analysis of 134 core from the Castlegate Sandstone, a braided fluvial system, and from the Star Point Sandstone, a marine shoreface system, indicate that the sandstones have ample matrix porosity (10 to 25%) and intrinsic permeability (100–10,000 millidarcy (md)) to store and transmit groundwater (Fig. 15). However, low permeability of fifth-order bounding surfaces, which are common, greatly limits groundwater movement (Black, 2000). Fifth-order bounding surfaces define major channel bodies, the geometry of which can range from ribbon to sheet like. Such bodies may be laterally continuous for thousands of meters (Miall, 1988). Many of these bounding surfaces have horizontal permeability < 1 md, and all have vertical permeability < 10 md. All vertical permeability measurements were made on sand-dominated samples. Attempts to core mud-dominated fifth-order

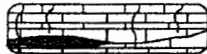

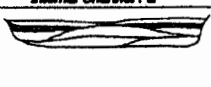
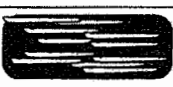

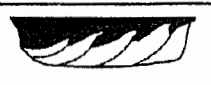
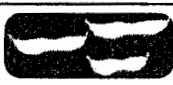


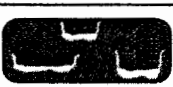


<i>Depositional System</i>				<i>2D Relations</i>	<i>Formations</i>
<i>Open/Marginal Lacustrine</i>					Flagstaff
<i>Fluvial Systems</i>		<i>Channel Geometry Map View</i>	<i>Geometry of Internal Channel Fill</i>		
	Bedded				Castlegate
	Mixed Load				Price River
	Suspended Load				North Horn, upper-middle Blackhawk
<i>Marine Shoreface and Foreshore</i>					lower Blackhawk, Star Point
<i>Open Marine Shale</i>					Mancos Shale

Figure 13. Depositional environments and internal structure of bedrock formations in Book Cliffs and Wasatch Plateau, Utah (modified from Galloway and Hobday, 1983).

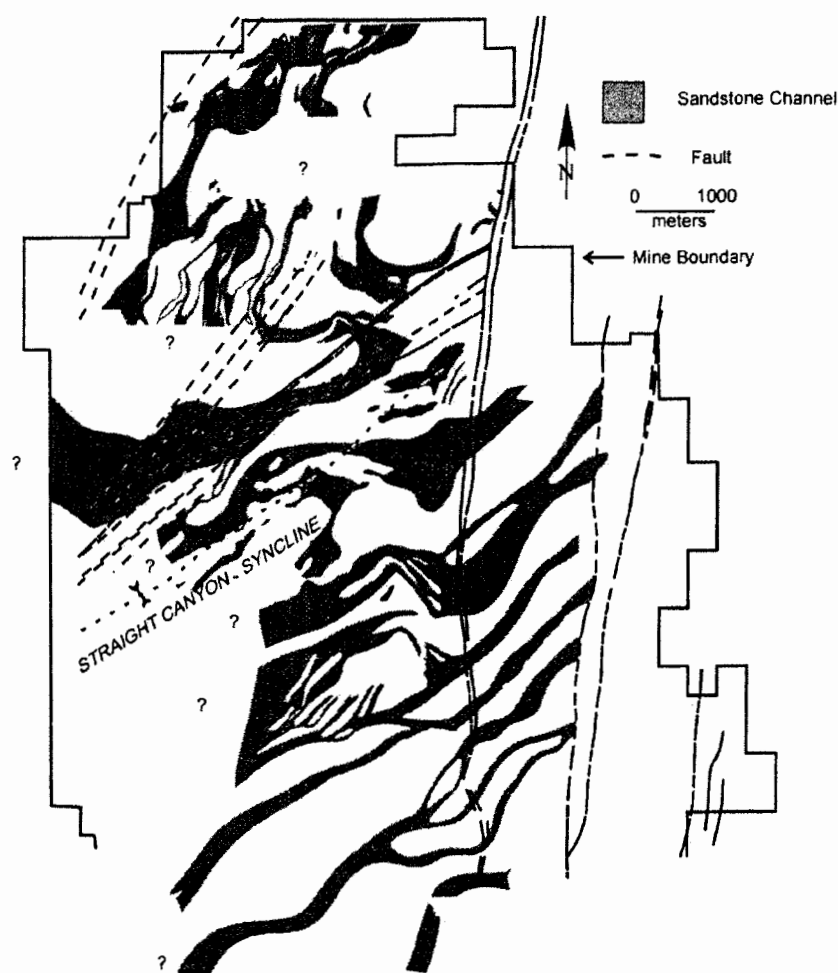


Figure 14. Map of lower Blackhawk Formation sandstone channel complex immediately above coal seams in Energy West Mine.

bounding surfaces vertically were unsuccessful due to core splitting. We assume that mud-dominated surfaces would have even lower permeability than sand-dominated surfaces.

The Star Point Sandstone is fundamentally different than the other sandstone bodies (Mail, 1988, 1993) in that it is a succession of laterally and vertically stacked parasequences (Fig. 16; Holman, 2001). Facies shifts create permeability baffles that restrict flow between beds and bed sets both vertically and laterally. Large-scale facies shifts create permeability barriers (marine shale = 0.1 md) between reservoir quality facies of juxtaposed parasequences (Fig. 16). Horizontal permeabilities also vary greatly by facies. Average horizontal permeabilities are 220 md (foreshore), 93 md (upper shoreface), 52 md (middle shoreface), and only 4 md (lower shoreface). Backshore facies, which underlie coal beds, have an average horizontal permeability of 63 md. The large permeability differences explain aquifer partitioning commonly observed in in-mine monitoring wells.

Matrix-flow seepage velocities were calculated for the Castlegate and Star Point Sandstones based on core-plug permeability and the measured density of fifth-order bounding surfaces. On average, two to four fifth-order bounding surfaces occur horizontally every 100 m in fluvial sandstones of the Castlegate Sandstone. Assuming two fifth-order bounding surfaces per 100 m, with a permeability of 1 md and a width of 7.6 cm (based on core plug lengths), then 1.5 m of low-permeability rock exists for every 1000 m of aquifer. Conservative seepage calculations for the Castlegate Sandstone, assuming a unit gradient and a 5% specific retention, predict it would require 106 yr for groundwater to travel through 1000 m of aquifer; 56 yr to cross the fifth-order bounding surfaces and an additional 50 yr to travel the remaining 998.5 m. Similar calculations indicate that it would take ~284 and 506 yr for water to travel 1 km in the best reservoir quality Star Point Sandstone facies (foreshore and upper shoreface, respectively). A single surface of extremely low permeability would significantly increase travel times. Because many horizontal travel distances are more than 1 km and the reservoir-quality sandstones are not laterally continuous, these calculated long travel times for optimal aquifer

TABLE 6. AVERAGE $\delta^2\text{H}$ AND $\delta^{18}\text{O}$ COMPOSITIONS OF SURFACE AND GROUNDWATERS IN THE BOOK CLIFFS AND WASATCH PLATEAU, UTAH

	All samples			Streams			Springs			In-mine		
	n	$\delta^2\text{H}$ (‰)	$\delta^{18}\text{O}$ (‰)	n	$\delta^2\text{H}$ (‰)	$\delta^{18}\text{O}$ (‰)	n	$\delta^2\text{H}$ (‰)	$\delta^{18}\text{O}$ (‰)	n	$\delta^2\text{H}$ (‰)	$\delta^{18}\text{O}$ (‰)
Book Cliffs												
West Ridge Mine	26	-112.3	-14.8	9	-112.7	-14.8	17	-112.1	-14.7			
std.		5.8	0.8		4.6	0.5		6.5	0.9			
Soldier Creek Mine	15	-111.6	-15.6	4	-107.3	-14.8	3	-106.7	-15.1	8	-115.6	-16.1
std.		5.7	0.7		1.0	0.22		5.0	0.6		4.20	0.47
Willow Creek Mine	30	-115.2	-15.2	13	-115.6	-14.9	8	-117.7	-15.4	9	-112.3	-15.3
std.		4.6	0.5		5.3	0.7		2.8	0.4		3.5	0.4
Wasatch Plateau												
Skyline Mines	111	-126.9	-17.0	27	-124.2	-15.6	69	-126.6	-16.9	15	-134.1	-18.1
std.		4.7	0.6		3.4	0.4		3.3	0.3		5.4	0.5
Co-Op Mine	60	-122.3	-16.2	9	-117.6	-15.4	40	-122.6	-16.2	11	-125.5	-17.0
std.		5.5	0.8		4.0	0.6		5.4	0.7		4.2	0.2
Genwall Mine	84	-125.5	-16.5	20	-123.1	-16.1	26	-125.7	-16.6	15	-132.1	-17.6
std.		4.1	0.6		2.4	0.3		2.7	0.4		2.4	0.4
Energy West Mines	21	-126.9	-16.7				11	-127.2	-16.6	10	-125.9	-16.6
std.		3.4	0.5					3.8	0.6		3.0	0.4
SUFCO Mine	76	-119.2	-16.0	24	-116.1	-15.6	36	-118.8	-15.9	18	-124.8	-16.8
std.		6.3	0.9		7.4	1.0		4.7	0.6		4.0	0.6

Note: std.—standard deviation.

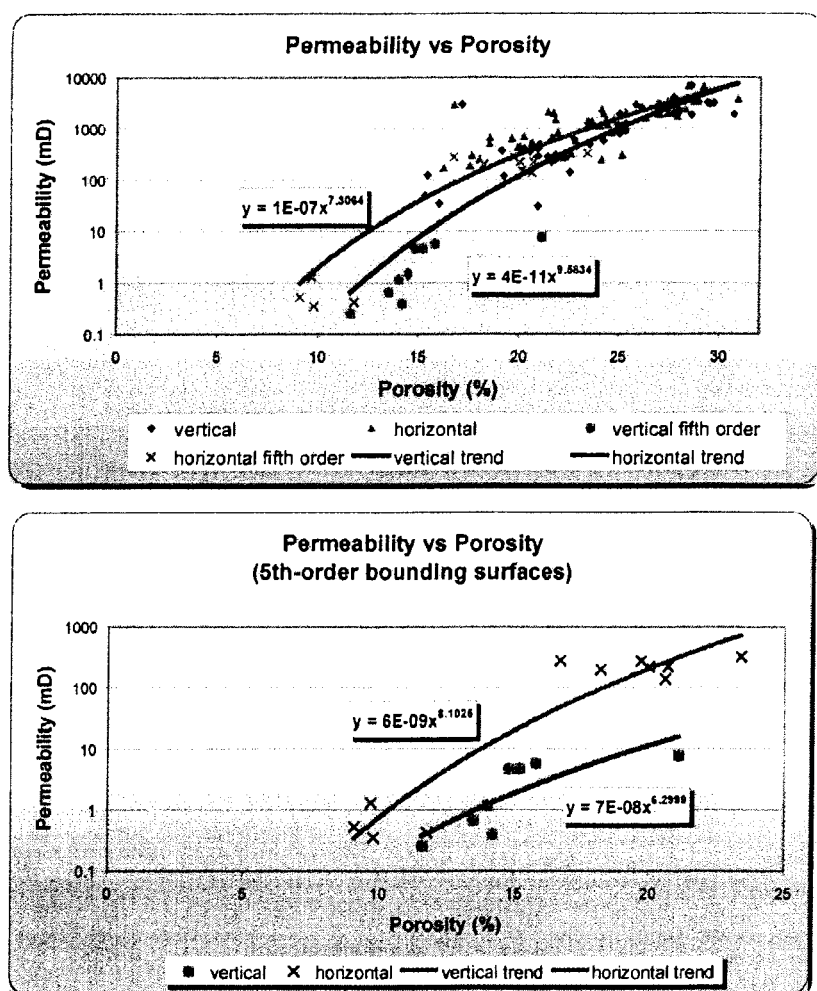


Figure 15. Scatter plots of permeability versus porosity from 120 cores of Castlegate Sandstone: A) all data, and B) fifth-order bounding surfaces only; md—millidarcy.

conditions are consistent with mean ^{14}C groundwater residence times of 500–20,000 yr.

Slow travel times in the Star Point Sandstone are confirmed by the ^{14}C ages of water in two wells completed at the Energy West Mine. The up-gradient and down-gradient wells have mean ^{14}C ages of 1000 and 6000 yr, respectively. Because geologic evidence suggests the two wells intercept groundwater along the same flow line, piston-flow travel times can be calculated using the method described by Mook (1980):

$$\Delta T = 8270 \ln (a_t^*/a_i^*) = 5,300 \text{ yr} \quad (1)$$

where:

ΔT is travel time (in years), a_t^* is ^{14}C activity

of up-gradient sample, a_i^* is ^{14}C activity of down-gradient sample.

Assuming a travel time of 5300 yr and a distance between the wells of 6.5 km, it takes ~ 960 yr to travel 1000 m.

Fault-related groundwater, with initial inflows as great as 325 l s^{-1} , have been encountered in the Soldier Creek, Skyline, Genwall, Energy West, and SUFCO Mines and are responsible for several notable springs in the Star Point Sandstone. These groundwaters issue from damage zones associated with the extensive network of high-angle normal faults (Fig. 2). In-mine discharge rates decline rapidly after initial encounter, and many completely cease. Groundwater ages of in-mine discharges are related to distance from cliff

faces and graben structures. Groundwater ages range from modern, containing measurable tritium, to 12,000 ^{14}C yr (Fig. 12). Young fault-related groundwater only occurs along fault reaches where the stress field associated with the outward expansion of cliff faces creates aperture in the damage zone that can communicate with the surface. Elsewhere along the damage zone, the fault water does not contain tritium and has older ^{14}C ages. Damage-zone groundwater is compartmentalized and does not readily recharge adjacent aquifer-quality rock. For example, in the Genwall Mine, water issuing from a fractured sandstone channel in the mine roof, located 100 m from the Joes Valley fault (Fig. 2), contained 0.95 TU, indicating hydraulic communication with surface water. Elsewhere, water in the roof channel sandstone, located near the fault, had 0 TU and older ^{14}C ages. Water issuing from the mining face, located ~ 60 m from the fault, also contained 0 TU and had a ^{14}C age of 2500 yr. Additionally, modern water in the damage zone did not impact the deeper Star Point Sandstone where a sample from a well, located ~ 60 m from the fault, contained 0 TU and had a ^{14}C age of 5000 yr.

Skyline Mine fault-related inflows that are located away from an outward expanding cliff face or major damage zone lack hydraulic communication with modern surface water. In-mine inflows of $\sim 325 \text{ l s}^{-1}$ persisted for more than six months from the extensive damage zone. In-mine samples had essentially 0 TU and ^{14}C ages of 6000 to 12,000 yr. Water from a surface well drilled into the fault zone had 0.17 TU (near the detection limit) and a ^{14}C age of 4600 (Fig. 12).

Two significant Star Point Sandstone springs (Big Bear and Birch, Figs. 4D and 5D) discharge water from parallel faults, which bound the Co-Op Mine. In Figure 4D, Big Bear is one of the three Star Point springs. Although the faults are only ~ 900 m apart and extend for several km, they do not have hydraulic communication with each other. Based on several sampling events at different sampling locations, Big Bear Spring discharge contains anthropogenic ^{14}C and has 14–17 TU. Birch Spring discharges a mixture of old water (^{14}C age of 1100 to 3600 yr) and modern water (0.33 to 1.13 TU; Fig. 12). The groundwater ages and seasonal and climatic responses indicate that Big Bear Spring discharges modern recharge water. Birch Spring mostly discharges older water and does not have seasonal responses, although it appears to respond to long-term climatic effects. Water from one in-mine Star Point Sandstone well has a ^{14}C age of 3000 yr, but contains 0.32 TU

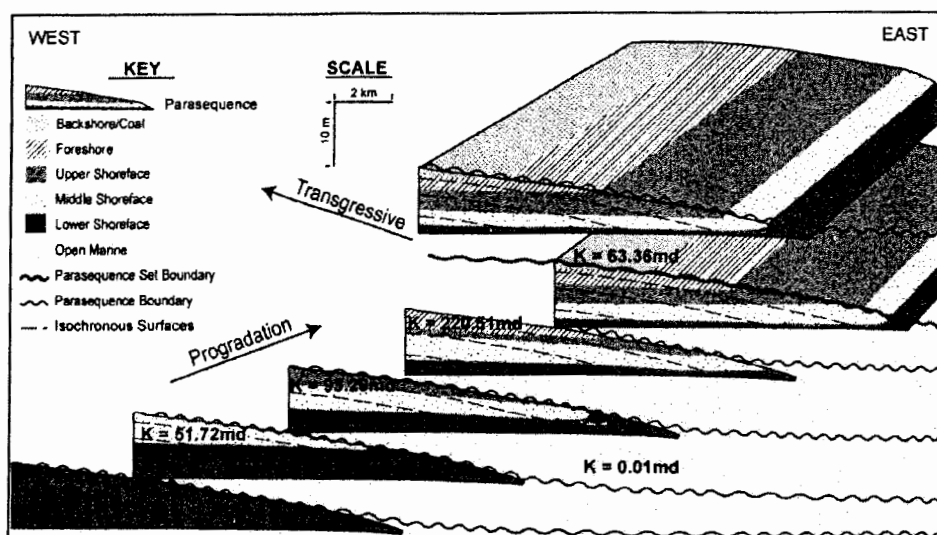


Figure 16. Schematic diagram of parasequences in Star Point Sandstone showing average horizontal permeability of Star Point sandstone facies. Diagram is not to scale; md—millidarcy.

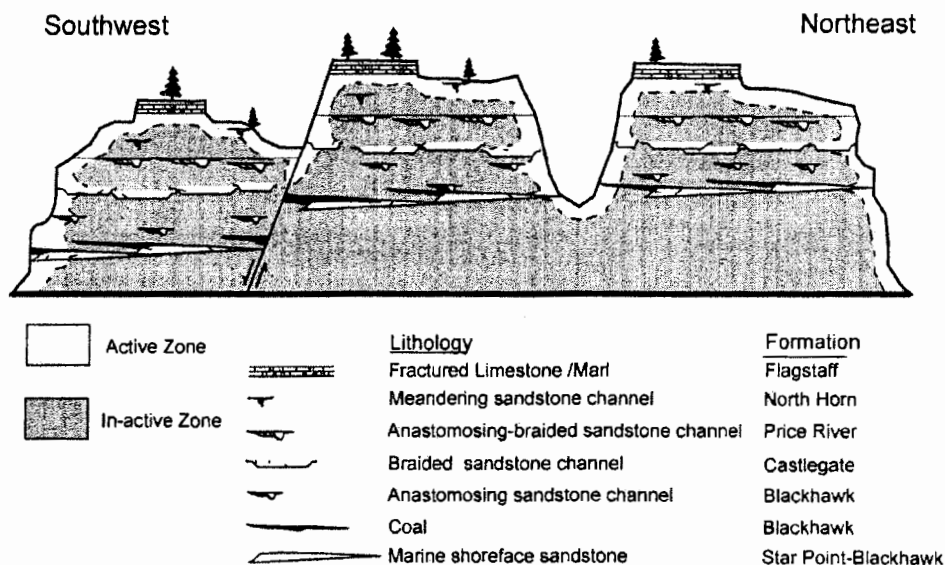


Figure 17. Conceptual model of hydrogeologic pathways. Active groundwater zone is exposed to meteoric water. Inactive groundwater zone is characterized by isolated reservoir quality sandstone disconnected from near-surface waters.

and therefore could have an affinity with Birch Spring. However, another nearby in-mine Star Point Sandstone well has a ^{14}C age of 900 yr and 0 TU.

DISCUSSION AND CONCLUSIONS

Two fundamentally different types of groundwater systems occur in the mountain-

ous terrain of the Wasatch Plateau and Book Cliffs: shallow and deep. Shallow-circulating groundwater is envisioned in the traditional sense of groundwater flow. Recharge water becomes progressively older as it moves in the subsurface along saturated flow paths until it ultimately discharges as springs and seeps. Shallow circulating, short flow-path systems respond rapidly to seasonal and climatic var-

iability. Locally, bedrock lithology controls solute compositions of the waters, but bedrock type does not control overall flow patterns.

Deep-circulating systems are encountered in mine openings as much as 700 m below ground surface. Most in-mine groundwater discharges from sandstone channels in mine roofs, although occasionally upwelling from the underlying Star Point Sandstone occurs.

In-mine hydrographs, $\delta^2\text{H}$ and $\delta^{18}\text{O}$ isotopic compositions, and ^{14}C groundwater "ages" demonstrate that deeply circulating groundwater systems have poor hydraulic communication with near-surface groundwater. These deep groundwater systems dewater fairly rapidly when encountered. Geochemical evolution modeling indicates that the potential for vertical migration of groundwater between the surface and bedrock formations and between bedrock formations is limited. This limited vertical migration suggests that appreciable recharge water tends to move laterally and down dip within the formation.

The two types of groundwater systems can be described by a simple conceptual model involving both active and inactive flow regimes (Fig. 17). The active regime includes all near-surface exposures, regardless of lithology. The near surface extends 75–150 m below ground surface and 150–300 m into cliff faces. Many mine entries are wet near the surface and all are dry at distances greater than ~150 m from the mine opening. In the active region, fractures with aperture, weathered rock, and matrix flow in fluvial sands control groundwater flow. Fault zones occasionally extend the active zone from the surface to deeper regions. The active zone is in direct hydraulic communication with seasonal recharge. Most open voids, including matrix and fractures, that are located below the vadose region are saturated.

The inactive zone includes most of the interior regions of the Wasatch Plateau and Book Cliffs, including most mine workings. Exploration drilling and in-mine test holes indicated that much of the void space, including matrix and fractures, is not water-saturated. In-mine groundwater occurs in both vertically and horizontally isolated fluvial channel sands that have limited hydraulic communication with the surface. Most groundwater inflow is restricted to aquifer-quality sandstones. Some channels are fully saturated and others are only saturated in their lower portions. When encountered in mine workings, these sandstone channels usually drain quickly. The coal seams, clays, and silts are barriers to vertical flow. This suggests fracture flow in a system of poorly connected fractures or relatively isolated regions of matrix flow. Permeability and porosity data suggest that groundwater ages in the Star Point and Castlegate Sandstones are consistent with matrix flow, limited by fifth-order bounding surfaces and facies bounding surfaces. The relationship between fracture and matrix flow is currently being investigated.

Fault-related groundwater flows occur in fault damage zones, and most deep fault-related

flow does not have rapid hydraulic communication with the surface. Rapid communication between the active zone and deep fault related flow, as evidenced by ^2H in the inactive zone, only exists where the stress field is such that fault-related fracture apertures can extend to surface as the result of outward expanding cliff faces or in complex fault damage zones.

Patterns of inactive zone groundwater flow do not occur in the traditional sense and are difficult to define. The ^{14}C ages of 20,000 yr or less suggest that groundwaters exist in slowly flowing systems (i.e., groundwater has finite ages). Yet, other data suggest that inactive zone groundwater occurs in discrete bodies that have extremely limited or no communication with annual recharge. Groundwater residence times have not been observed to progressively lengthen along plausible flow paths or become progressively older or younger as bodies of groundwater drain into mine openings. In the Wasatch Plateau and Book Cliffs, we suggest that recharge occurs during very wet climatic episodes and/or slowly along unsaturated fracture flow paths. Because inactive zone groundwater does not have an infinite age, it must discharge to the surface. Deep seepage is not plausible because of the thousands of feet of the very impermeable underlying Mancos Shale. Discharge locations and mechanism remain problematic. Only a few isolated springs, often fault-related and sometimes thermal, discharge old groundwater.

Beneath the coal horizons, the shoreface sandstones of the Star Point Sandstone are largely in the inactive zone and support groundwater flow. Generally, there is limited hydraulic communication between sand sheets. As with younger strata, active zone groundwater flow in the Star Point Sandstone is largely limited to fracture flow and the most significant flows are fault-zone related.

ACKNOWLEDGMENTS

This research has been funded by grants from the Utah Mining Association. We are particularly indebted to the mining companies and their staffs who provided us with company data, logistical support, underground access, and moral support. We thank the following companies and key personnel: Chuck Semborski (Energy West Mining Company), Chris Kravits, Wes Sorensen, and Ken May (SUFCO Mine), Chris Hansen, Gary Taylor, Barry Barnum, and Keith Zobel (Skyline Mine), Dave Spilman (Soldier Creek Mine), Johnny Papas (Willow Creek Mine), Charles Reynolds (Co-Op Mine), Wendel Koontz (West Elk Mine), and Jean Semborski, Gary Gray, and Dave Shaver (Genwal Mine and Andalex Resources).

We also thank John Sharp, Daniel Larson, Steve

Nelson, and an unknown reviewer for their thoughtful reviews, criticisms, and comments regarding the manuscript.

REFERENCES CITED

- Allen, D.M., and Michel, 1998, Evaluation of multi-well test data in a faulted aquifer using linear and radial flow models: *Groundwater*, v. 36, p. 938–948.
- Black, B.J., 2000, Fluid flow characterization of the Castlegate Sandstone, Southern Wasatch Plateau, Utah: Interpretation of reservoir porosity through permeability and porosity analysis (M.S. thesis): Provo, Utah, Brigham Young University, 145 p.
- Chan, M.A., and Phaff, B.J., 1991, Fluvial sedimentology of the upper Cretaceous Castlegate Sandstone, Book Cliffs, Utah: *Utah Geological Association Publication* 19, p. 95–109.
- Committee on Fracture Characterization and Fluid Flow, 1996: Rock fractures and fluid flow: Contemporary understandings and applications: Washington, D.C., National Academy of Sciences, 551 p.
- Fontes, J.Ch., and Garmier, J.M., 1979, Determination of the initial ^{14}C activity of the total dissolved carbon: A review of existing models and a new approach: *Water Resources Research*, v. 15, p. 399–413.
- Forster, C., and Smith, L., 1988, Groundwater flow systems in mountainous terrain. 2. Controlling factors: *Water Resources Research*, v. 24, p. 1011–1023.
- Franczk, J.K., and Pitman, J.K., 1991, Latest Cretaceous non-marine depositional systems in the Wasatch Plateau area: Reflections of foreland to inter-montane basin transition: *Utah Geological Association Publication* 19, p. 77–93.
- Freeze, R.A., and Witherspoon, P.A., 1966, Theoretical analysis of regional groundwater flow I. Analytical and numerical solutions to the mathematical model: *Water Resources Research*, v. 2, p. 641–656.
- Freeze, R.A., and Witherspoon, P.A., 1967, Theoretical analysis of regional groundwater flow II. Effects of water table configuration and subsurface permeability variations: *Water Resources Research*, v. 3, p. 623–634.
- Galloway, W.E., and Hobday, D.K., 1983, Terrigenous clastic depositional systems: Applications to petroleum, coal, and uranium exploration: New York, Springer-Verlag, p. 71.
- Garner, A., and Morris, T.H., 1996, Outcrop study of the lower Green River Formation for reservoir characterization and hydrocarbon production enhancement in the Altamont-Bluebell Field, Uinta Basin, Utah: *Utah Geological Survey, Miscellaneous Publication* 96-2, 61 p.
- Hintze, L.F., 1988, Geologic history of Utah: *Brigham Young University Geology Studies Special Publication* 7, 203 p.
- Holman, L.S., 2001, The effect of parasequence geometry and facies architecture on reservoir partitioning of the Star Point Sandstone, Wasatch Plateau, Utah [M.S. thesis]: Provo, Utah, Brigham Young University, 156 p.
- Hubbert, M.K., 1940, The theory of groundwater motion: *Journal of Geology*, v. 48, p. 785–944.
- Huntoon, P.W., 1981, Fault controlled ground-water circulation under the Colorado River, Marble Canyon, Arizona: *Ground Water*, v. 19, p. 20–27.
- Jamieson, G.R., and Freeze, R.A., 1983, Determining hydraulic conductivity distribution in a mountainous area using mathematical modeling: *Ground Water*, v. 21, p. 168–177.
- Janes, S.D., 1998, Anisotropic groundwater migration in structurally deformed sedimentary bedrock terrains: *American Association of Petroleum Geologists Bulletin*, v. 81, p. 849–850.
- Johnson, J.L., 1978, Stratigraphy of the coal-bearing Blackhawk Formation on North Horn Mountain, Wasatch Plateau, Utah: *Utah Geology*, v. 5, p. 57–77.
- Kamola, D.L. and Huntoon, J.E., 1995, Repetitive stratigraphic patterns in a foreland basin sandstone and their

- possible tectonic significance: *Geology*, v. 23, p. 177-180.
- Knowles, S.P., 1983, Geology of the Scofield 7.5 minute quadrangle in Carbon, Emery and Sanpete Counties, Utah: *Brigham Young Geology Studies*, v. 32, p. 85-100.
- Lines, G.C., 1985, The ground-water system and possible effects of underground coal mining in the Trail Mountain area, Central Utah: U.S. Geological Survey Water Supply Paper 2259, 32 p.
- Mayer, J.R., and Sharp, J.M. Jr., 1998, Fracture control of regional ground-water flow in a carbonate aquifer in a semi-arid region: *Geological Society of America Bulletin*, v. 110, no. 2, p. 269-283.
- Mayo, A.L., and Koontz, W., 2000, Fracture flow and groundwater compartmentalization in the Rollins Sandstone, lower Mesa Verde Group, Colorado, USA: *Hydrogeology Journal*, v. 8, p. 430-446.
- Mayo, A.L., Muller, A.B., and Ralston, D.R., 1985, Hydrogeochemistry of the Meade thrust allochthon south-eastern Idaho, and its relevance to the stratigraphic and structural groundwater flow control: *Journal of Hydrology*, v. 76, p. 27-61.
- Mayo, A.L., Petersen, E.C., and Kravits, C., 2000, Chemical evolution of coal mine drainage in a non-acid producing environment, Wasatch Plateau, Utah: *Journal of Hydrology*, v. 236, p. 1-16.
- Miall, A.D., 1988, Reservoir heterogeneities in fluvial sandstones: Lessons from outcrop studies: *American Association of Petroleum Geologists Bulletin*, v. 72, p. 682-697.
- Miall, A.D., 1993, The architecture of fluvial-deltaic sequences in the upper Mesa Verde Group (Upper Cretaceous), Books Cliffs, Utah, in Best, L.L., and Barstow, C.S., eds., *Braided rivers: Geological Society [London] Special Publication 75*, p. 305-332.
- Mook, W.G., 1980, Carbon-14 in hydrogeologic studies, in Fritz, P., and Fontes, J.C., eds., *Handbook of environmental isotope hydrogeochemistry*, v. 1: The terrestrial environment: Amsterdam, Elsevier, p. 49-74.
- Morris, T.H., and Mayo, A.L., 2000, Hierarchical scale and variety of hydrogeologic barriers and baffles in stratified heterolithic terrain, Wasatch Plateau, Utah: *Geological Society of America Abstracts with Programs*, v. 32, no. 7, p. A-411.
- National Climatic Data Center, 2001a, National Climatic Data Center online monthly climatic parameters: www.ncdc.noaa.gov/coop-precip.html (March 2001).
- National Climatic Data Center, 2001b, National Climatic Data Center online monthly climatic parameters: www.ncdc.noaa.gov/pub/data/cirs/drought/README (March 2001).
- Ostle, B., and Malone, L.C., 1988, *Statistics in research* (fourth edition): Ames, Iowa, Iowa State University Press, 666 p.
- Pearson, F.J., Jr., Bedinger, M.S., and Jones, B.F., 1972, Carbon-14 dates of water from Arkansas Hot springs, in *Proceeding of eighth international conference on radiocarbon dating*: Wellington, Royal Society of New Zealand, v. 1, p. 330-247.
- Plummer, L.N., Prestmon, E.C., and Parkhurst, D.L., 1991, NETPATH—An interactive code (NETPATH) for modeling net geochemical reactions along a flow path: U.S. Geological Survey Water Resources Investigation 91-4078, 94 p.
- Stanley, K.O., and Colinson, J.W., 1979, Depositional history of Paleocene-lower Eocene Flagstaff Limestone and coeval rocks, central Utah: *American Association of Petroleum Geologists Bulletin*, v. 63, p. 311-323.
- Toth, J., 1962, A theory of groundwater motion in small drainage basins in central Alberta: *Journal of Geophysical Research*, v. 67, p. 4375-4387.
- Toth, J., 1963, A theoretical analysis of groundwater flow in small drainage basins: *Journal of Geophysical Research*, v. 68, p. 4795-4812.
- Utah State University Climate Center, 2001, Online data for Emery, Huntington, Castledale, Salina and Scofield Dam weather station: www.climate.usu.edu/free/USA_UT.HTM (March 2001).
- Van Wagoner, J.C., Mitchum, R.M., Campion, K.M., and Rahmanian, V.D., 1990, *Siliciclastic sequence stratigraphy in well logs, cores, and outcrops: Concepts for high-resolution correlation of time and facies*: Houston, Texas, American Association of Petroleum Geologists Methods in Exploration Series, v. 42, p. 558-571.
- Western Region Climate Center, 2001, Desert Research Institute online precipitation data: www.wrcc.dri.edu/climsmut.html (March 2001).
- Witkind, I.J., and Weiss, M.P., 1991, Geologic map of the Nephi 30' x 60' Quadrangle, Carbon, Emery, Juab, Sanpete, Utah, and Wasatch Counties, Utah: U.S. Geological Survey Miscellaneous Investigations Series Map I-1937, scale 1:100,000, 1 sheet.

MANUSCRIPT RECEIVED BY THE SOCIETY 6 MARCH 2002

REVISED MANUSCRIPT RECEIVED 13 JANUARY 2003

MANUSCRIPT ACCEPTED 21 FEBRUARY 2003

Printed in the USA